

The role of titanium oxide concentration profile of titanium oxide of RuO₂-TiO₂ coatings obtained by the sol-gel procedure on its electrochemical behavior

VLADIMIR V. PANIĆ^{1*#}, ALEKSANDAR B. DEKANSKI^{1#}, VESNA B. MIŠKOVIĆ-STANKOVIĆ^{2#},
SLOBODAN K. MILONJIĆ^{3#} and BRANISLAV Ž. NIKOLIĆ^{2#}

¹ICTM–Center of Electrochemistry, University of Belgrade, Njegoševa 12, P.O. Box 473, 11001 Belgrade,

²Faculty of Technology and Metallurgy, University of Belgrade, Karnegijeva 4, P.O. Box 3503, 11120 Belgrade and ³Vinča Institute of Nuclear Sciences, P.O. Box 522, 11001 Belgrade, Serbia and Montenegro

(Received 1 August 2003)

Abstract: In order to understand the role of TiO₂ in the deactivation mechanism of an active RuO₂-TiO₂ coating, an additional TiO₂ layer was introduced in the support/coating interphase of regular Ti/[RuO₂-TiO₂] anode in one case and on the surface of the coating in the other. The electrochemical behavior of these, with TiO₂ enriched, anodes was compared with the behavior of anodes with regular RuO₂-TiO₂ coatings, which were subjected to an accelerated stability test. A high-frequency semicircle in the complex plane plot, obtained by electrochemical impedance spectroscopy, for a regular RuO₂-TiO₂ coating corresponds to TiO₂ enrichment in the coating as a consequence of anode corrosion. In the case of the coatings with additional TiO₂ layers, a high-frequency semicircle was not observed. The additional TiO₂ layers increase the coating overall resistance and influence the coating impedance behavior at low frequencies. Similar equivalent electrical circuits were used to analyze the impedance behavior of coatings having an additional TiO₂ layer at different position within RuO₂-TiO₂ coating.

Keywords: RuO₂-TiO₂ coating, corrosion stability, oxide sols, sol-gel procedure, electrochemical impedance spectroscopy.

INTRODUCTION

Dimensionally stable anodes lose their electrocatalytic activity during long-term electrolysis, which leads to the end of their service life of an anode. Corrosion stability, *i.e.*, anode service life, can be monitored by an accelerated stability test (AST),^{1–4} which is based on the galvanostatic electrolysis of a dilute chloride solution at relatively high current density. In the AST, the end of the service life of an anode is seen as a sudden increase of the potential at constant current, which is caused by an increase in the coating resistance. The increase in resistance could be a consequence of the growth of an insulating TiO₂ layer in

* Corresponding author.

Serbian Chemical Society active member.

the substrate|coating interphase, caused by the oxidation of the Ti substrate, and/or by the anodic dissolution of catalytically active Ru species, which enriches the coating surface with insulating TiO₂. An erosion of the coating can also be involved in this deactivation pathway.^{1,5} The anode deactivation mechanism depends on the coating morphology. In earlier works,^{4,6} Ti/[RuO₂-TiO₂] anodes with considerably different service life were obtained by changing the conditions in the sol-gel procedure for the coating preparation, which resulted in oxide particles of different size and, consequently, differences in the coating morphology. Also, sol-gel prepared anodes have considerably longer service life than corresponding anodes prepared by the thermal decomposition of ruthenium and titanium chloride.^{3,4}

Electrochemical impedance spectroscopy (EIS) can provide useful information on the deactivation mechanism of oxide coatings.^{2,7-9} The appearance of a semicircle in the high frequency domain of a complex plane plot indicates the loss of the electrocatalytic activity of the RuO₂-TiO₂ coating.⁹ The resistance related to this semicircle does not depend on the electrode potential at which the EIS data were collected, but does depend on the employed electrolyte and its conductivity.⁹ Boots and co-workers^{2,7} registered similar impedance behavior for corroded RuO₂-IrO₂ and RuO₂-Co₃O₄ coatings.

From our earlier results⁹ and literature data,^{2,7} it is not clear whether the insulating TiO₂ layer, which causes the appearance of a semicircle, grows in the Ti substrate|coating interphase and/or on the surface of the corroded coating. The aim of this work was to investigate the influence of the concentration profile of titanium oxide in the RuO₂-TiO₂ coating on the electrochemical behavior of the anode, which should provide useful information about the anode deactivation mechanism.

EXPERIMENTAL

Preparation of anodes

The forced hydrolysis of chloride salts in extremely acid aqueous solutions at boiling temperature was used to prepare RuO₂ and TiO₂ sols.^{3,4} The solutions were aged for 46 h (RuO₂ sol preparation) and 30 h (TiO₂ sol preparation), in order to obtain the coating with the best characteristics.⁴ The oxide sols were mixed in amounts to produce a coating composition of 40 % at. Ru-60 %at. Ti. To prepare the regular RuO₂-TiO₂ coating, an appropriate amount of the mixture of sols, which would produced an amount of coating of 0.5 mg cm⁻² counted to the binary oxide, was applied onto titanium plates (2 cm × 2 cm × 1 mm). After drying at 70 °C in air, whereby a gel phase is formed on the surface, the sample was calcined at 450 °C in air. The additional TiO₂ layer in the substrate|coating interphase of a regular Ti/[RuO₂-TiO₂] anode was obtained by application of the appropriate amount of TiO₂ sol (to produce an amount of 0.3 mg cm⁻² of TiO₂) and thermal treatment under the same temperature regime. A TiO₂ layer on the coating surface was obtained in the same manner. Consequently, the notations of the investigated anodes are: Ti/[RuO₂-TiO₂], Ti/TiO₂/[RuO₂-TiO₂] and Ti/[RuO₂-TiO₂]/TiO₂. In some experiments, two TiO₂ layers were formed on the active RuO₂-TiO₂ coating surface.

Accelerated stability test of Ti/[RuO₂-TiO₂] anode

The AST of the Ti/[RuO₂-TiO₂] anode was performed by electrolysis of 0.5 mol dm⁻³ NaCl, pH 2, at a constant current density of 400 mA cm⁻² and a temperature of 25 °C, in a cell with a Pt plate counter electrode. The changes in the anode potential were recorded during the AST. A sudden increase of the potential implies that the anode can no longer be used in practice (the end of service life). Illustration of an AST is given in Fig. 1.

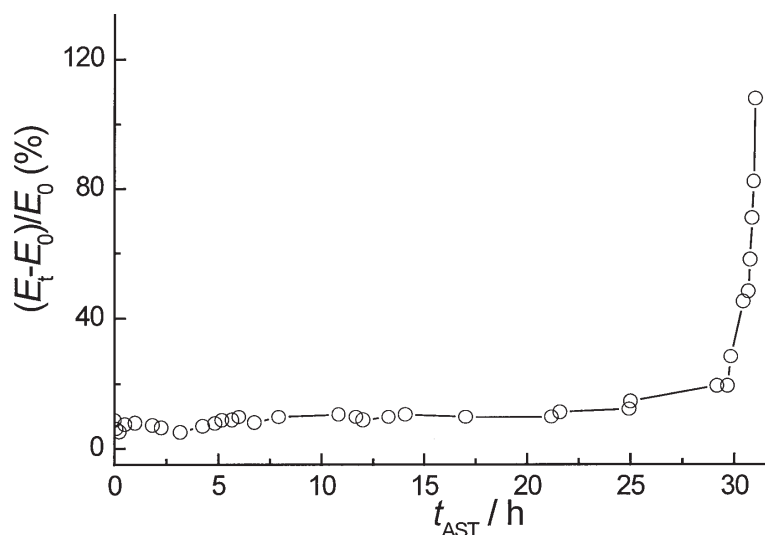


Fig. 1. Accelerated stability test of a regular Ti/RuO₂-TiO₂ anode. Electrolyte: 0.5 mol dm⁻³ NaCl, pH 2; temperature: 25 °C; current density: 400 mA cm⁻².

Investigation of anode properties

The electrochemical properties of Ti//TiO₂/[RuO₂-TiO₂] and Ti//[RuO₂-TiO₂]/TiO₂ anode as well as the properties of Ti//[RuO₂-TiO₂] anode before and after AST were investigated by cyclic voltammetry (CV) and EIS in 1 mol dm⁻³ HClO₄ and by polarization measurements in 0.5 mol dm⁻³ NaCl, pH 2. The cell was equipped with a magnetic stirrer, a Pt plate as counter electrode and a saturated calomel electrode (SCE) as the reference electrode. All potentials are expressed on the SCE scale. The impedance data were recorded using a 5 mV amplitude of sinusoidal voltage around the potential of 1.25 V over a frequency range of 100 kHz to 50 mHz and analyzed using a suitable fitting procedure.¹⁰ The experiments were performed at room temperature.

RESULTS AND DISCUSSION

Cyclic voltammetry

The cyclic voltammograms of a fresh (before AST) Ti//[RuO₂-TiO₂] anode, a corroded (after AST) Ti//[RuO₂-TiO₂] anode, a Ti//TiO₂/[RuO₂-TiO₂] and a Ti//[RuO₂-TiO₂]/TiO₂ anode are shown in Fig. 2. Within the potential window of electrolyte stability, the voltammograms are of similar shape, which is characteristic for the pseudocapacitive behavior of this type of electrode material.¹¹ The anodes with an additional TiO₂ layer seem to be more active for hydrogen evolution than the regular Ti//[RuO₂-TiO₂] anode. The voltammogram of the corroded anode and of the anodes containing an additional TiO₂ layer are tilted due to the considerable resistance of the coating, indicating the greater resistance of the Ti//TiO₂/[RuO₂-TiO₂] compared to the Ti//[RuO₂-TiO₂]/TiO₂ anode. This means that a more compact TiO₂ layer is formed in the interphase than on the coating surface. The insulating TiO₂ layer on the coating surface covers the active sites on the surface, but the inner active sites (in pores and cracks) are still active. The capacitive behavior is related to the inner active sites

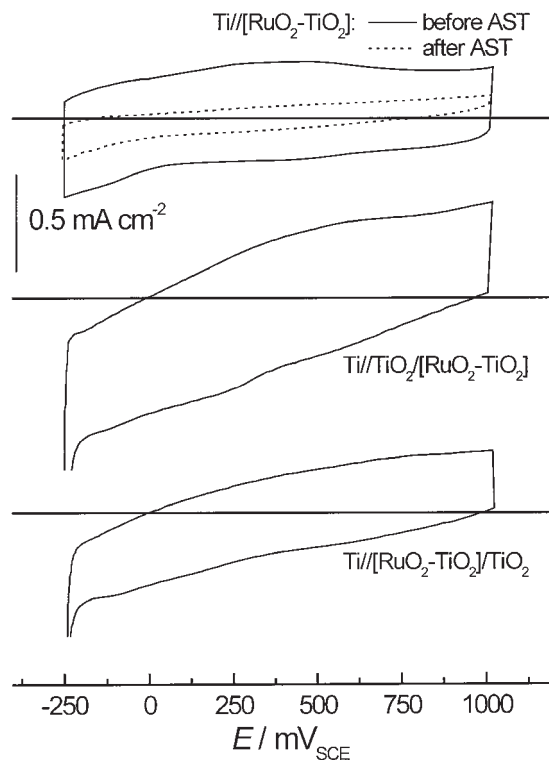


Fig. 2. Cyclic voltammograms of the $\text{Ti} // [\text{RuO}_2\text{-TiO}_2]$ anode recorded before and after AST and of the $\text{Ti} // \text{TiO}_2 / [\text{RuO}_2\text{-TiO}_2]$ and $\text{Ti} // [\text{RuO}_2\text{-TiO}_2] / \text{TiO}_2$ anode. Electrolyte: $1 \text{ mol dm}^{-3} \text{ HClO}_4$, room temperature. Sweep rate: 20 mV s^{-1} .

with capacitance and pore resistance in series. The number of active sites accessible to the electrolyte, *i.e.*, the electrochemically active surface area,⁴ corresponds to the surface area under the anodic part of the voltammograms. The apparent anodic charge densities, in mC cm^{-2} , obtained from the voltammograms for fresh $\text{Ti} // [\text{RuO}_2\text{-TiO}_2]$, corroded $\text{Ti} // [\text{RuO}_2\text{-TiO}_2]$, $\text{Ti} // \text{TiO}_2 / [\text{RuO}_2\text{-TiO}_2]$ and $\text{Ti} // [\text{RuO}_2\text{-TiO}_2] / \text{TiO}_2$ anode are 12.25, 3.05, 13.10 and 8.72, respectively. A considerably smaller anodic charge is registered for the corroded $\text{Ti} // [\text{RuO}_2\text{-TiO}_2]$ anode when compared to the others. This indicates a decrease in the number of active sites due to the continuous dissolution of Ru species during the AST. The additional TiO_2 layer in the substrate|coating interphase does not significantly affect the anodic charge, but a lower value is registered for the anode with the TiO_2 layer on the coating surface. These effects are expected, since insulating TiO_2 on the surface covers the active RuO_2 species but does not affect those species if it is placed in the interphase.

Polarization measurements

$E\text{-log } j$ plots of the investigated anodes are shown in Fig. 3. The plots have been corrected for the pseudo-ohmic voltage drop by the IR compensation procedure given for the PAR 273A potentiostat, used for the CV and polarization measurements. It should be mentioned that the resistance values required for the IR compensation followed the order:

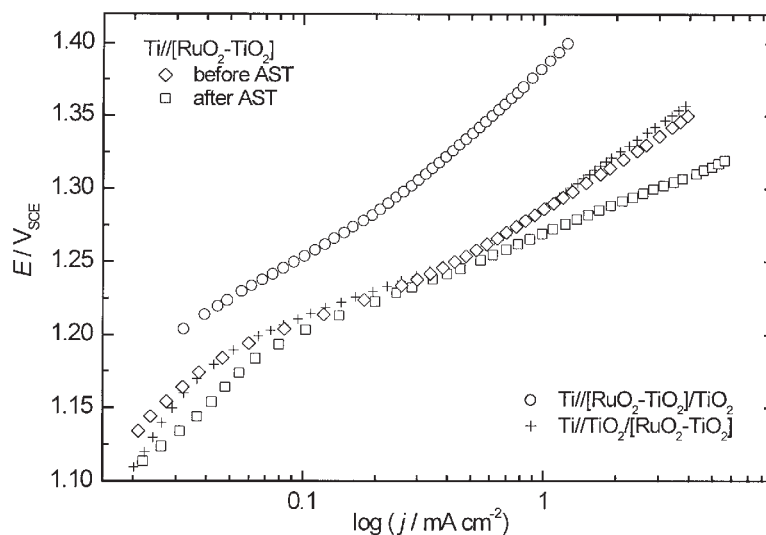


Fig. 3. E - $\log j$ characteristics of the Ti//[RuO₂-TiO₂] anode recorded before and after AST, and of the Ti/TiO₂/[RuO₂-TiO₂] and Ti//[RuO₂-TiO₂]/TiO₂ anode. Electrolyte: 0.5 mol dm⁻³ NaCl, pH 2; room temperature.

Ti//[RuO₂-TiO₂] < corroded Ti//[RuO₂-TiO₂] < Ti//[RuO₂-TiO₂]/TiO₂ << Ti/TiO₂/[RuO₂-TiO₂], indicating the increased value of the coating resistance after the AST and by addition of the TiO₂ layers, particularly by the layer in the substrate|coating interphase.

Regardless the kinetics and mechanism of the processes occurring on the anode, it is obvious that the Ti//[RuO₂-TiO₂]/TiO₂ anode shows the worst polarization characteristics, while the Ti/TiO₂/[RuO₂-TiO₂] and Ti//[RuO₂-TiO₂] anode behave similarly. It seems strange that the corroded Ti//[RuO₂-TiO₂] anode shows good polarization characteristics, even better than the others in the region of higher current density. Although most of the electrocatalytically active RuO₂ species were dissolved during the AST, there are still enough active sites for a current (considerably smaller than the current used in the AST) to pass. The coating is more porous after the AST, the surface area is large and this effect overcomes the effect of RuO₂ dissolution. This statement can be supported by the fact that the overpotential decreases exponentially with the thickness of the porous layer, which is a feature known from the theory of porous electrodes.¹² Since the dissolution of Ru species during the AST produces a coating with a more porous structure, the active sites of the corroded Ti//[RuO₂-TiO₂] anode situated deeper in the bulk of the coating became involved in the reaction. On the contrary, the polarization data of the Ti//[RuO₂-TiO₂] anode before the AST should relate to the active sites situated closer to the surface of the coating. It was found earlier that the number of active sites in the bulk of the coating is greater than on the coating surface due to surface enrichment in TiO₂ during the thermal formation of the coating.¹

Electrochemical impedance spectroscopy

The complex plane plots shown in Fig. 4 illustrate the impedance behavior of the prepared anodes in the oxygen evolution reaction. Figure 4a shows the EIS data collected over the whole frequency range (100 kHz–50 mHz), while Fig. 4b shows the high-frequency part of the plots from Fig. 4a. The lines in Fig. 4 give the results of the fitting procedure.

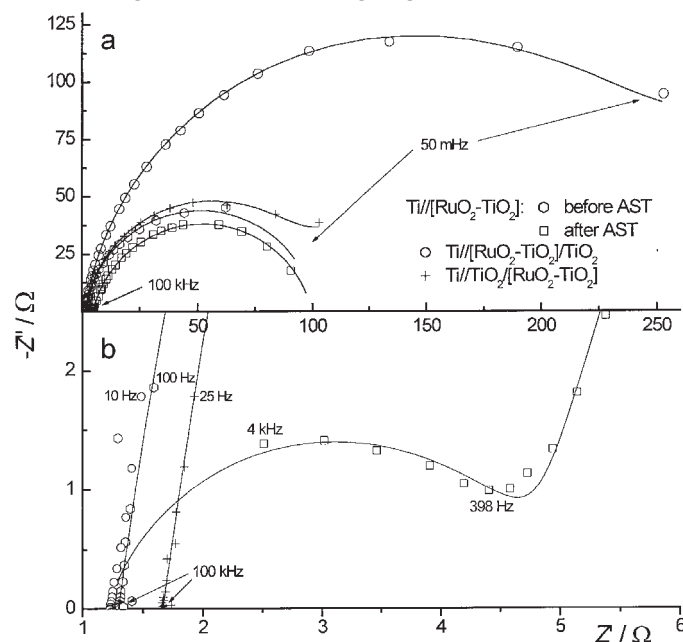


Fig. 4. The impedance complex plane plots of the $\text{Ti}/[\text{RuO}_2\text{-TiO}_2]$ anode recorded before and after AST, and of the $\text{Ti}/\text{TiO}_2/[\text{RuO}_2\text{-TiO}_2]$ and $\text{Ti}/[\text{RuO}_2\text{-TiO}_2]/\text{TiO}_2$ anode over the whole frequency range (a) and in the high frequency range (b). Potential: 1.25 V, electrolyte: 1 mol dm^{-3} HClO_4 , room temperature.

The anode deactivation by the AST is manifested by the appearance of high-frequency semicircle in the EIS plot for the corroded $\text{Ti}/[\text{RuO}_2\text{-TiO}_2]$ anode (Fig. 4b). Similar behavior was observed in an earlier work,⁹ and also by other authors.^{7,8} It was shown that the coating pore resistance, related to the high-frequency semicircle, depends on the electrolyte conductivity but not on the electrode potential.⁹ Figure 4a also shows that anode corrosion results in no significant changes in the characteristics of the semicircle related to charge transfer across the solution/coating interphase at lower frequencies.

Differences in the EIS behavior of the $\text{Ti}/\text{TiO}_2/[\text{RuO}_2\text{-TiO}_2]$ and $\text{Ti}/[\text{RuO}_2\text{-TiO}_2]$ anode are seen at high and low frequencies. Since the somewhat higher value of the electrolyte resistance of $\text{Ti}/\text{TiO}_2/[\text{RuO}_2\text{-TiO}_2]$ anode should rather be ascribed to experimental error, the main difference in their EIS behavior is registered at low frequencies. A considerably greater charge transfer semicircle is obtained for the $\text{Ti}/[\text{RuO}_2\text{-TiO}_2]/\text{TiO}_2$ anode, which again confirms the considerably smaller number of active sites that exchange charge with the electrolyte.

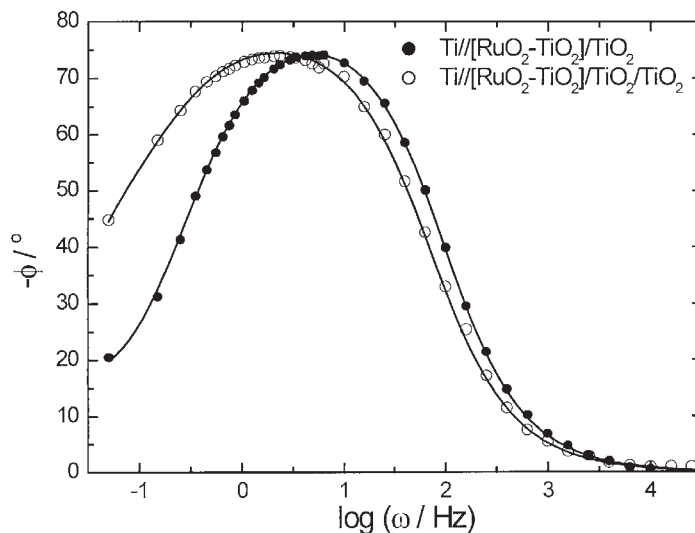


Fig. 5. Bode phase angle plots of the anodes with different amount of TiO₂ inserted at the coating surface. EIS data recorded in 1 mol dm⁻³ HClO₄ at a potential of 1.25 V.

As can be seen in Fig. 4b, there is no evidence of a well-pronounced high-frequency semicircle in the plots of the EIS data for the anodes with an additional TiO₂ layer. This indicates that the morphology of the additional layer is different to that formed during anode deactivation. Also, the morphology of the additional TiO₂ layer depends on the position of the layer with respect to the RuO₂-TiO₂ coating, which causes a difference in the anode impedance behavior. Concerning the anode with the TiO₂ layer on the coating surface, there is no significant difference in impedance behavior at high frequencies if the amount of TiO₂ on the coating surface is doubled (two additional layers: Ti//[RuO₂-TiO₂]/TiO₂/TiO₂), as illustrated by the Bode phase angle plots in Fig. 5. On the contrary, the differences in the low-frequency domain became more pronounced with increased amount of TiO₂ at the coating surface.

Equivalent electrical circuits

The simple equivalent electrical circuit (EEC) with the inscription $R_{\Omega}(R_{ct}Q)$,¹⁰ where R_{Ω} is the solution resistance, R_{ct} is the charge transfer resistance across the active site/solution interphase, and Q is a constant phase element related to the coating capacitance, was sufficient to describe the impedance behavior of a freshly prepared Ti//[RuO₂-TiO₂] anode. In order to describe the anode impedance behavior after AST, additional elements, which represent the pore resistance, R_p , of TiO₂ layer formed during anode deactivation and Q_L , related to the TiO₂ layer capacitance, were included in the EEC: $R_{\Omega}(R_pQ_L)(R_{ct}Q)$.

The values of the parameters of the EEC elements are given in Table I. There are no considerable changes in the R_{ct} values, nor in the values of the parameters Y_0 and n for Q , which is consistent with the results and conclusions from polarization

measurements. The charge transfer resistance is lower for the corroded anode, while the capacitance is higher. This is opposite to the CV results, which indicates that EIS “can see” deeper into the coating bulk than CV at the applied sweep rate. The unique feature caused by anode deactivation is the appearance of the $R_p Q_L$ combination.

The EECs which describe the impedance behavior of the anodes with an additional TiO_2 layer in the substrate|coating interphase and two TiO_2 layers on the coating surface are similar to the EEC of the corroded $\text{Ti}/[\text{RuO}_2\text{-TiO}_2]$ anode. The same elements as in the case of the corroded anode constitute the EEC for $\text{Ti}/[\text{RuO}_2\text{-TiO}_2]/\text{TiO}_2/\text{TiO}_2$, where R_p is the pore resistance of the additional TiO_2 layers. The circuit inscription for $\text{Ti}/\text{TiO}_2/[\text{RuO}_2\text{-TiO}_2]$ anode is $R_\Omega(R_L Q_L)(R_{ct} Q)$, where R_L is the resistance of the TiO_2 layer instead of R_p . Contrary to the corroded anode, the semicircles related to the additional TiO_2 layers and that related to charge transfer are highly overlapped and cannot be separately seen in the plots in Fig. 4. In the case of the $\text{Ti}/[\text{RuO}_2\text{-TiO}_2]/\text{TiO}_2$ anode, there is no evidence of the formation of a separate TiO_2 layer, and EEC is $R_\Omega(Q_{dl}(R_{ct}(Q_p)))$, where Q_p is a constant phase element related to the pseudocapacitance of RuO_2 . This EEC indicates that the addition of TiO_2 on the coating surface enables the pseudocapacitance to be distinguished from the double layer capacitance, which is a known impedance feature of $\text{RuO}_2\text{-TiO}_2$ coatings with low RuO_2 content.¹¹ The obtained Y_0 value of Q_p (Table I) is of the same order of magnitude as the capacitance that can be calculated from the voltammogram shown in Fig. 2 ($10^{-2} \text{ F cm}^{-2}$). This consideration indicates that the TiO_2 on the coating surface is highly doped with RuO_2 migrating from the neighboring $\text{RuO}_2\text{-TiO}_2$ layer during thermal treatments.

The values of the EEC parameters for the anodes with additional TiO_2 can be seen in Table I. The R_L value obtained for $\text{Ti}/\text{TiO}_2/[\text{RuO}_2\text{-TiO}_2]$ is considerably higher than the R_p value obtained for the corroded $\text{Ti}/[\text{RuO}_2\text{-TiO}_2]$ anode, while the Y_0 value of Q_L for the latter is considerably lower. Even so, the Y_0 value of Q_L for $\text{Ti}/\text{TiO}_2/[\text{RuO}_2\text{-TiO}_2]$ is quite similar to the Y_0 value of Q obtained for fresh and corroded $\text{Ti}/[\text{RuO}_2\text{-TiO}_2]$ anodes, which indicates the doping effect from the neighboring $\text{RuO}_2\text{-TiO}_2$ layer, like in the case of the $\text{Ti}/[\text{RuO}_2\text{-TiO}_2]/\text{TiO}_2$ anode. This consideration leads to the conclusion that the R_L value should not be considerably higher than the value of R_p for the corroded anode, which suggests the formation of TiO_2 in the substrate|coating interphase as the cause for deactivation of sol-gel prepared anodes is less probable. On the other hand, the Y_0 value of Q_L obtained for the $\text{Ti}/[\text{RuO}_2\text{-TiO}_2]/\text{TiO}_2/\text{TiO}_2$ anode is closer to the value obtained for the corroded anode than to the value for $\text{Ti}/\text{TiO}_2/[\text{RuO}_2\text{-TiO}_2]$ anode, while the R_p value is three orders of magnitude higher than for the corroded anode. This is due to the considerably greater compactness of the additional TiO_2 layers in the $\text{Ti}/[\text{RuO}_2\text{-TiO}_2]/\text{TiO}_2/\text{TiO}_2$ anode. The high compactness of the TiO_2 layer is also seen through the R_{ct} value registered for the $\text{Ti}/[\text{RuO}_2\text{-TiO}_2]/\text{TiO}_2/\text{TiO}_2$ anode being the highest, since the active sites are hardly accessible for the species involved in the charge transfer process.

TABLE I. The values of the equivalent electrical circuit parameters for the investigated anodes

Parameter	Anode				
	Ti//[RuO ₂ -TiO ₂]		Ti/TiO ₂ [RuO ₂ -TiO ₂]	Ti//[RuO ₂ -TiO ₂]/TiO ₂	Ti//[RuO ₂ -TiO ₂]/TiO ₂ /TiO ₂
	Before AST	After AST			
EEC:	$R_{\Omega}(R_{ct}Q)$	$R_{\Omega}(R_pQ_L)(R_{ct}Q)$	$R_{\Omega}(R_LQ_L)(R_{ct}Q)$	$R_{\Omega}(Q_{dl}(R_{ct}(Q_p))$	$R_{\Omega}(R_pQ_L)(R_{ct}Q)$
R_{Ω}/Ω	1.7	1.8	1.8	1.6	2.0
R_p/Ω	–	3.9	–	–	1283
R_L/Ω	–	–	168	–	–
Q_L	Y_0/Ω^{-1}	1.6×10^{-5}	3.2×10^{-3}	–	4.1×10^{-4}
n	–	0.77	0.82	–	0.91
R_{ct}/Ω	103	96	150	264	347
Q	Y_0/Ω^{-1}	3.5×10^{-3}	4.7×10^{-3}	–	3.8×10^{-3}
n	0.91	0.87	0.96	–	0.87
Q_{dl}	Y_0/Ω^{-1}	–	–	2.4×10^{-3}	–
n	–	–	–	0.91	–
Q_p	Y_0/Ω^{-1}	–	–	4.6×10^{-2}	–
n	–	–	–	0.63	–

The impedance behavior of the investigated anodes indicates that the loss of electrocatalytic activity of sol-gel prepared anodes is due to the formation of a TiO₂ layer on the coating surface rather than to the growth of a TiO₂ layer at the substrate|coating interphase.

CONCLUSION

Regular Ti//[RuO₂-TiO₂] anodes and anodes with additional TiO₂ layers in the substrate|coating interphase and on the coating surface were investigated by cyclic voltammetry, polarization measurements and electrochemical impedance spectroscopy. Cyclic voltammetry experiments showed a decrease in the electrochemically active surface area during corrosion of the RuO₂-TiO₂ coating and an increase in the coating resistance. The coating resistance is also increased by additional TiO₂ layers, particularly by a layer in the substrate|coating interphase. Similar conclusions about the coating resistance resulted from polarization measurements, but they indicated an increase in the porosity of the coating during anode corrosion. The mechanism of the deactivation of the Ti//[RuO₂-TiO₂] anode during long-term electrolysis is seen in its impedance behavior as the appearance of a high-frequency semicircle, as the consequence of TiO₂ enrichment in the coating. The data obtained by EIS measurements for the anode with two additional TiO₂ layers on the coating surface show similarity to the EIS data of the corroded Ti//[RuO₂-TiO₂] anode. The conclusion appears to be that the loss of anode activity of sol-gel prepared Ti//[RuO₂-TiO₂] anode is dominantly due to an enrichment of the coating surface with TiO₂ which remains after RuO₂ dissolution.

Acknowledgements: This research is financially supported by the Ministry of Science, Technology and Development, Republic of Serbia, Project No. 1230.

ИЗВОД

УЛОГА КОНЦЕНТРАЦИОНОГ ПРОФИЛА ТИТАН-ОКСИДА У
ЕЛЕКТРОХЕМИЈСКОМ ПОНАШАЊУ RuO₂-TiO₂ ПРЕВЛАКА ДОБИЈЕНИХ
СОЛ-ГЕЛ ПОСТУПКОМ

ВЛАДИМИР В. ПАНИЋ¹, АЛЕКСАНДАР Б. ДЕКАНСКИ¹, ВЕСНА Б. МИШКОВИЋ-СТАНКОВИЋ²,
СЛОБОДАН К. МИЛОЊИЋ³ и БРАНИСЛАВ Ж. НИКОЛИЋ²

¹ИХТМ - Центар за електрохемију, Њеџошева 12, бр. 815, 11000 Београд,

²Технолошко-металуршки факултет, Карнегијева 4, бр. 3503, 11120 Београд и

³Институт за нуклеарне науке "Винча", бр. 522, 11001 Београд

У циљу испитивања улоге титан-оксида у деактивацији RuO₂-TiO₂ превлаке на титанској подлози, испитиване су особине анода са додатним слојем TiO₂ у међуфази подлога/превлака, односно на површини превлаке. Електрохемијско понашање ових упоређено је са понашањем анода са уобичајеном RuO₂-TiO₂ превлаком, као и са онима које су биле подвргнуте убрзаном тесту стабилности. Појава полукруга у високо-фреквентној области у дијаграмима у комплексној равни, која је регистрована спектроскопијом електрохемијске импеданције за уобичајене RuO₂-TiO₂ превлаке, а која је последица обогаћивања превлаке са TiO₂ током њене деактивације, није уочена код анода са додатим TiO₂ слојем. Додати TiO₂ слојеви повећавају омску отпорност превлаке и утичу на импеданцијско понашање при ниским фреквенцијама. За анализу импеданцијског понашања превлака са додатим TiO₂ слојевима као и уобичајених RuO₂-TiO₂ превлака које су деактивирани коришћена су слична еквивалентна електрична кола.

(Примљено 1. августа 2003)

REFERENCES

1. V. M. Jovanović, A. Dekanski, P. Despotov, B. Nikolić, R. T. Atanasoski, *J. Electroanal. Chem.* **339** (1992) 147
2. V. A. Alves, L. A. Silva, J. F. C. Boodts, *J. Appl. Electrochem.* **28** (1998) 899
3. V. Panić, A. Dekanski, S. Milonjić, R. Atanasoski, B. Nikolić, *Colloids Surfaces A* **157** (1999) 259
4. V. Panić, A. Dekanski, S. Milonjić, R. Atanasoski, B. Nikolić, *Electrochim. Acta* **46** (2000) 415
5. A. Dekanski, V. M. Jovanović, P. Despotov, B. Nikolić, R. T. Atanasoski, *J. Serb. Chem. Soc.* **56** (1991) 167
6. D. Mitrović, V. Panić, A. Dekanski, S. Milonjić, R. Atanasoski, B. Nikolić, *J. Serb. Chem. Soc.* **66** (2001) 847
7. L. M. Da Siolva, L. A. De Faria, J. F. C. Boodts, *J. Electroanal. Chem.* **532** (2002) 141
8. T. A. F. Lassali, J. F. C. Boodts, L. O. S. Bulhões, *J. Appl. Electrochem.* **30** (2000) 625
9. V. Panić, V. Mišković-Stanković, A. Dekanski, S. Milonjić, B. Nikolić, *The European Corrosion Congress, EUROCORR 2001*, Riva del Garda, Lake Garda, Italy, October 2001, CD-ROM, Paper No. 097
10. B. Boucamp, *Equivalent Circuit (EQUIVCRT.PAS) Users Manual*, Univ. Twente, Enschede, The Netherlands, 1989
11. B. Conway, *Electrochemical Supercapacitors – Scientific Fundamentals and Technological Applications*, Plenum Publishers, New York, 1999, p. 259
12. Yu. Chizmadzev, Yu. Chirkov in *Comprehensive Treatise of Electrochemistry Vol. 6*, E. Yeager, J. Bockris, B. Conway, S. Sarangapani, Eds., Ch. 5, Plenum Press, New York, 1983.